

Cation disorder in ferroelectric Aurivillius phases of the type $\text{Bi}_2\text{ANb}_2\text{O}_9$ (A = Ba, Sr, Ca)

Susan M. Blake, Mark J. Falconer, Mark McCreedy and Philip Lightfoot*

School of Chemistry, University of St Andrews, St Andrews, Fife, UK KY16 9ST

The structures of the ferroelectric two-layer Aurivillius phases $\text{Bi}_2\text{ANb}_2\text{O}_9$ (A = Ba, Sr, Ca) have been refined using a combination of X-ray and neutron powder diffraction data. $\text{Bi}_2\text{BaNb}_2\text{O}_9$ is not significantly distorted from idealised symmetry and has been refined in tetragonal space group $I4/mmm$, $a = 3.9362(1)$ and $c = 25.6582(7)$ Å. The Sr and Ca compounds have been refined in orthorhombic space group $A2_1am$, with $a = 5.5193(3)$, $b = 5.5148(3)$, $c = 25.0857(6)$ Å and $a = 5.4833(1)$, $b = 5.4423(1)$, $c = 24.8984(6)$ Å, respectively. The orthorhombic distortion increases with decreasing A^{2+} cation size and originates from bonding requirements at the perovskite A site, in agreement with previous work. However, in contrast to earlier work, we find a partial mixing of Bi and A cations on their respective sites, which increases in the order $\text{Ca} < \text{Sr} < \text{Ba}$. This effect is also discussed in terms of bonding requirements at the metal sites and bond valence sum analysis. The combined use of X-ray and neutron powder diffraction data is found to be essential in determining this subtle effect, which may have important consequences in the interpretation of the ferroelectric behaviour of this family of materials.

The Aurivillius phases¹ are a class of layered bismuth oxides, which may be described structurally as intergrowths of fluorite-like $(\text{Bi}_2\text{O}_2)^{2+}$ layers with perovskitic $(\text{A}_{n-1}\text{B}_n\text{O}_{3n+1})^{2-}$ layers ($n = 1, 2, 3, 4$), typical examples being Bi_2WO_6 , $\text{Bi}_2\text{SrTa}_2\text{O}_9$ and $\text{Bi}_4\text{Ti}_3\text{O}_{12}$. They have been well known as ferroelectric materials since the pioneering work of Smolenski *et al.*² and Subbarao,³ who extensively studied their ferroelectric properties as a function of composition. However, it has only been recently that serious crystallographic studies have been carried out on these materials in an attempt to correlate ferroelectric properties with detailed structural effects. Thus the structures of the three-layer phase $\text{Bi}_4\text{Ti}_3\text{O}_{12}$ ⁴ and the two-layer phases $\text{Bi}_3\text{TiNbO}_9$ ⁵ and $\text{Bi}_2\text{SrTa}_2\text{O}_9$ ⁶ have now been analysed thoroughly and it has been shown that earlier work on these materials was incorrect. There is clearly a need for a reappraisal of much of the earlier interpretation of the ferroelectric behaviour of these materials and a corresponding need for additional detailed crystallographic studies in order to further our understanding of these systems. This need has been exacerbated by the recent exciting developments in non-volatile computer memory applications using thin films of $\text{Bi}_2\text{SrTa}_2\text{O}_9$ as an information storage medium. $\text{Bi}_2\text{SrTa}_2\text{O}_9$ has been shown to have significantly improved properties for these applications over the existing $\text{Pb}(\text{Zr},\text{Ti})\text{O}_3$ based systems.⁷ The work of Withers and co-workers^{4-6,8} has suggested that the major cause of spontaneous polarisation in the two-layer materials is the displacement of the A site cation in the perovskite block along the a -direction in the polar space group $A2_1am$ and not the movement of the B site cation away from the octahedral centre. In the light of this, an accurate determination of the crystal structure of these phases is essential in order that the environment around each cation site is precisely known. A further important question regards the possibility of anti-site defects on the cation sublattice, *i.e.* Bi on the A site and A on the bismuth site in the systems $\text{Bi}_2\text{AB}_2\text{O}_9$ (A = Ba, Sr, Ca; B = Nb, Ta). This possibility was first suggested, without crystallographic evidence, by Smolenski *et al.*² in order to rationalise the broadened ferroelectric transition in $\text{Bi}_2\text{BaNb}_2\text{O}_9$. Recent work by Ismunandar *et al.*⁹ using powder neutron diffraction data suggested that there was no cation site disordering in these systems, however a similar study of $\text{Bi}_2\text{PbNb}_2\text{O}_9$ by Srikanth *et al.*¹⁰ suggested that some disorder may be present. In addition, the solid solution $\text{Bi}_{2-x}\text{Pb}_x\text{SrNb}_2\text{O}_9$ has been reported by Millan *et al.*¹¹ which suggests that Pb^{2+} at least

may substitute for Bi^{3+} in the (Bi_2O_2) layers. In order to readdress these problems we have carried out a detailed study of the system, $\text{Bi}_2\text{AB}_2\text{O}_9$ (A = Ca, Sr, Ba) by combined X-ray and neutron powder diffraction methods. The complementarity of X-ray and neutron scattering allows a more precise and unambiguous refinement to be carried out and we show for the first time that metal anti-site defects of this type do indeed occur in these systems.

Experimental

Stoichiometric amounts of Bi_2O_3 , Nb_2O_5 and the appropriate alkaline-earth carbonate were ground together, pelleted and heated at 700 °C for 12 h. The $\text{Bi}_2\text{SrNb}_2\text{O}_9$ sample was heated for 12 h at both 900 and 1000 °C, with grinding and repelleting after each heating stage. The $\text{Bi}_2\text{BaNb}_2\text{O}_9$ and $\text{Bi}_2\text{CaNb}_2\text{O}_9$ samples were heated at 1000 °C for 24 h and then a further 12 h with an intermediate grinding. All samples were slow cooled in air.

Powder X-ray diffraction data were collected on a Stoe Stadi P automated diffractometer equipped with a small position sensitive detector, using monochromatised $\text{Cu-K}\alpha_1$ radiation. Data were collected over the range of $10^\circ < 2\theta < 90^\circ$ in 0.02° steps, the entire run lasting about 15 h. Appropriate absorption corrections were applied by measuring the transmission factors of the samples at $2\theta = 0$. Powder neutron diffraction data were collected from 5–8 g samples on the SEPD instrument¹² at the intense pulsed neutron source at Argonne National Laboratory. Data analysis was carried out by the Rietveld method using the GSAS program suite.¹³

Structure refinement

Examination of both the X-ray and neutron data indicated that $\text{Bi}_2\text{BaNb}_2\text{O}_9$ was tetragonal with absences compatible with space group $I4/mmm$. Despite the fact that the ferroelectric Curie temperature of $\text{Bi}_2\text{BaNb}_2\text{O}_9$ was reported as 200 °C by Subbarao,³ attempts to refine the structure in the polar space group $A2_1am$ were unsuccessful, hence it was assumed that no significant distortions from idealised symmetry occurred. The structure reported for $\text{Bi}_2\text{PbNb}_2\text{O}_9$ by Aurivillius¹ was adapted and used as a starting model for the refinement and it was assumed that the cations were fully ordered, *i.e.* Ba occupying the A site only. Initially, only the X-ray data were used to

refine this model. In addition to the usual profile and atomic parameters, a preferred orientation parameter along [001] was refined. At this stage of the refinement, the agreement factors were, $R_{wp}=9.68\%$, $R_p=6.83\%$ and $\chi^2=2.036$ and the value of the bismuth thermal parameter was noticeably higher than the barium thermal parameter [$U_{iso}(\text{Bi})=0.066$ and $U_{iso}(\text{Ba})=0.037$]. The barium and bismuth atoms were then allowed to be disordered, but the temperature factors of these atoms were constrained to be equal. One parameter was refined to describe the disorder, such that both sites were fully occupied and the Bi:Ba stoichiometry was maintained. An improvement in the fit of the model was then evident and R_{wp} , R_p , and χ^2 all decreased to 8.63%, 6.10% and 1.620, respectively. After this stage the neutron data were added and a joint refinement was carried out. The final Rietveld plots for the neutron and X-ray refinements are shown in Fig. 1(a) and (b), respectively. We believe that this model, with the temperature factors of the two Bi/A sites being constrained to be equal, represents the most valid model for a system of this nature. We are attempting to account for disorder of two dissimilar atoms on each site, and due to the lone-pair effect of Bi^{3+} the local environment around each site may be quite different. For this reason we think it inappropriate to refine two separate temperature factors for these sites. However, results of refinements of this type are included in Tables 1–4, for comparison.

$\text{Bi}_2\text{SrNb}_2\text{O}_9$ and $\text{Bi}_2\text{CaNb}_2\text{O}_9$ were both found to be orthorhombic and refinements were carried out in space group $A2_1am$ using an adaptation of the model reported by Withers *et al.*⁵ Withers used an unconventional setting of $A2_1am$ which made the structure more comparable to the idealised $Fmmm$ version. The addition of $(\frac{1}{2}, \frac{1}{2}, 0)$ to the atomic coordinates reported by Withers reverted the model to a conventional setting of the space group. The same sequence of refinement was followed as in the $\text{Bi}_2\text{BaNb}_2\text{O}_9$ refinement, but the x coordinate of the bismuth site was fixed, in order to define the origin of the polar axis. In both compounds, disordering of the alkaline earth cation and the bismuth cation resulted in a

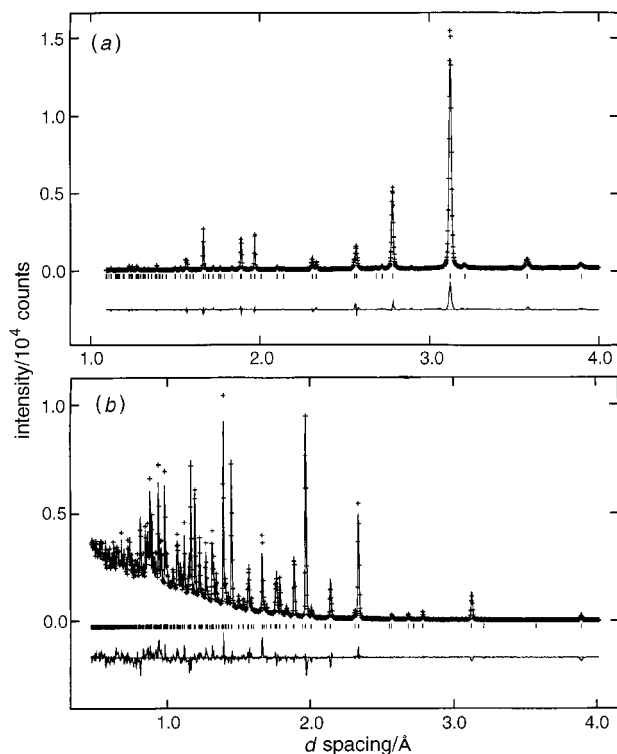


Fig. 1 Final Rietveld fit for $\text{Bi}_2\text{BaNb}_2\text{O}_9$ using (a) X-ray data and (b) neutron data. Crosses represent observed data, the solid line is the calculated pattern; the difference profile and allowed reflection positions are shown beneath.

visible improvement of the fit of the model and a corresponding reduction in the values of R_{wp} , R_p and χ^2 . Again, refinements with and without the temperature factor constraint on the Bi/A sites are were carried out, and the results presented in Tables 2–4. The final Rietveld plots for the neutron and X-ray refinements of $\text{Bi}_2\text{SrNb}_2\text{O}_9$ and $\text{Bi}_2\text{CaNb}_2\text{O}_9$ are shown in Fig. 2(a) and (b), and Fig. 3(a) and (b), respectively.

Results and Discussion

The structures of three Aurivillius phases, $\text{Bi}_2\text{BaNb}_2\text{O}_9$, $\text{Bi}_2\text{SrNb}_2\text{O}_9$ and $\text{Bi}_2\text{CaNb}_2\text{O}_9$ have been refined using powder X-ray and neutron diffraction data, simultaneously. The final refined atomic parameters of these structures are presented in Tables 1–3. The details of the structure refinements are presented in Table 4. The structures of the idealised $\text{Bi}_2\text{BaNb}_2\text{O}_9$ and the distorted $\text{Bi}_2\text{CaNb}_2\text{O}_9$ are shown in Fig. 4(a) and (b), respectively.

It can be seen from Table 4, that the orthorhombic distortion of the unit cell increases as the A site cation size decreases. In this study, $\text{Bi}_2\text{BaNb}_2\text{O}_9$ was treated as tetragonal, whereas a recent neutron diffraction study by Ismunandar *et al.*⁹ reported an orthorhombic structure for this phase. The present diffraction data showed no evidence for lowering of symmetry from body-centred tetragonal, although the room-temperature phase is reported to be ferroelectric.

$\text{Bi}_2\text{BaNb}_2\text{O}_9$, $\text{Bi}_2\text{SrNb}_2\text{O}_9$ and $\text{Bi}_2\text{CaNb}_2\text{O}_9$ all exhibited disordering between the perovskite A site cation and the bismuth cation in the Bi_2O_2 layer. This was true for both the models presented, with each type of refinement showing the same trends across the series Ba–Sr–Ca. Discussion will now address the refinements with constrained Bi/A temperature factors only. The proportion of cation disorder decreased as the size of the A site cation decreased, *i.e.* $\text{Bi}_2\text{BaNb}_2\text{O}_9$ had 13.4% barium on the bismuth site in the Bi_2O_2 layer, whereas $\text{Bi}_2\text{CaNb}_2\text{O}_9$ had only 5.3% calcium on this site. The structural study by Ismunandar *et al.*⁹ on $\text{Bi}_2\text{BaNb}_2\text{O}_9$ and $\text{Bi}_2\text{SrNb}_2\text{O}_9$ found no evidence of this cation disorder, but the reported temperature factors of the bismuth cation were much higher than the barium or strontium cation. This difference in temperature factors also existed in our refinements, until the cations were allowed to disorder. It should be noted that Ismunandar *et al.*⁹ did not include X-ray diffraction data in their refinement and used a different sample preparation method. X-Ray data are much more sensitive to the cation disorder (neutron scattering lengths are $\text{Bi}=0.853 \times 10^{-12}$ cm, $\text{Ba}=0.525 \times 10^{-12}$ cm, $\text{Sr}=0.702 \times 10^{-12}$ cm and $\text{Ca}=0.490 \times 10^{-12}$ cm).

There is only one reported structure refinement in which cation disordering was observed and this was on the $\text{Bi}_2\text{PbNb}_2\text{O}_9$ phase,¹⁰ using powder neutron data. The degree of cation disorder was attributed to the cooling treatment of the sample during synthesis. Slow cooled samples exhibited more cation disorder than quenched samples, but the errors reported for the occupancies of the Pb and Bi sites were very high. The effect of different cooling rates on the samples has not been investigated in this study.

The only other report of possible cation disorder was by Smolenski *et al.*² who noted that the phase transition of $\text{Bi}_2\text{BaNb}_2\text{O}_9$ was broader than $\text{Bi}_2\text{SrNb}_2\text{O}_9$, and tentatively attributed this to the Ba and Bi atoms disordering.

Since the samples in this study were all cooled in the same way, the degree of cation disorder should be considered to be a direct consequence of the variation in A site cation size. It is perhaps surprising that the largest sized A site cation compound (Ba) displays the most cation disorder. It would normally be expected that the largest cation would prefer to completely occupy the larger A site rather than partially occupy both the A site and the smaller, more distorted 'bismuth' site. The smaller cations (*i.e.* Sr and Ca) would

Table 1 Refined model of Bi₂BaNb₂O₉ from XRD and neutron data^a

atom	site	x	y	z	occupancy	<i>U</i> _{iso}
Ba(1)	2b	0.5(—)	0.5(—)	0.0(—)	0.732(11) ^{1,b}	0.0396(5) ²
Bi(1)	2b	0.5(—)	0.5(—)	0.0(—)	0.268(11) ^b	0.0396(5)
Ba(2)	4e	0.5(—)	0.5(—)	0.20310(7)	0.134(5) ^b	0.0396(5) ³
Bi(2)	4e	0.5(—)	0.5(—)	0.20310(7)	0.866(5) ^b	0.0396(5)
Nb	4e	0.0(—)	0.0(—)	0.08860(7)	1.0(—)	0.0036(3)
O(1)	2a	0.5(—)	0.5(—)	0.5(—)	1.0(—)	0.032(1)
O(2)	4d	0.0(—)	0.5(—)	0.25(—)	1.0(—)	0.0082(6)
O(3)	4e	0.0(—)	0.0(—)	0.1603(1)	1.0(—)	0.0202(7)
O(4)	8g	0.0(—)	0.5(—)	0.07818(7)	1.0(—)	0.0126(5)

^aAlternative model (see text), 1: 0.57(2), 2: 0.055(2), 3: 0.0335(8). ^bRestraints used (see text).

Table 2 Refined model of Bi₂SrNb₂O₉ from XRD and neutron data^a

atom	site	x	y	z	occupancy	<i>U</i> _{iso}
Sr(1)	4a	0.274(2)	0.751(1)	0.5(—)	0.787(8) ^{1,b}	0.0308(5) ²
Bi(1)	4a	0.274(2)	0.751(1)	0.5(—)	0.213(8) ^b	0.0308(5)
Sr(2)	8b	0.25(—) ^c	0.7354(6)	0.70155(7)	0.106(4) ^b	0.0308(5) ³
Bi(2)	8b	0.25(—) ^c	0.7354(6)	0.70155(7)	0.894(4) ^b	0.0308(5)
Nb	8b	0.269(1)	0.2549(8)	0.58668(7)	1.0(—)	0.0042(5)
O(1)	4a	0.310(2)	0.212(2)	0.5(—)	1.0(—)	0.007(2)
O(2)	8b	0.284(2)	0.302(1)	0.6589(2)	1.0(—)	0.020(1)
O(3)	8b	0.523(2)	0.494(1)	0.2489(2)	1.0(—)	0.0042(7)
O(4)	8b	0.523(2)	0.519(1)	0.5706(1)	1.0(—)	0.0023(5)
O(5)	8b	0.578(1)	0.046(1)	0.5850(2)	1.0(—)	0.0023(5)

^aAlternative model (see text), 1: 0.866(8), 2: 0.0125(9), 3: 0.0392(7). ^bRestraints used (see text). ^cPosition not refined, in order to define origin along *a*.

Table 3 Refined model of Bi₂CaNb₂O₉ from XRD and neutron data^a

atom	site	x	y	z	occupancy	<i>U</i> _{iso}
Ca(1)	4a	0.262(2)	0.750(1)	0.5(—)	0.895(4) ^{1,b}	0.0298(5) ²
Bi(1)	4a	0.262(2)	0.750(1)	0.5(—)	0.105(4) ^b	0.0298(5)
Ca(2)	8b	0.25(—) ^c	0.7287(3)	0.70056(6)	0.053(2) ^b	0.0298(5) ³
Bi(2)	8b	0.25(—) ^c	0.7287(3)	0.70056(6)	0.947(2) ^b	0.0298(5)
Nb	8b	0.2816(7)	0.2495(6)	0.58439(7)	1.0(—)	0.0052(4)
O(1)	4a	0.327(1)	0.174(1)	0.5(—)	1.0(—)	0.001(1)
O(2)	8b	0.297(1)	0.3147(7)	0.6560(2)	1.0(—)	0.016(1)
O(3)	8b	0.507(1)	0.5010(7)	0.2488(2)	1.0(—)	0.0030(6)
O(4)	8b	0.513(1)	0.5397(8)	0.5630(2)	1.0(—)	0.0081(5)
O(5)	8b	0.609(1)	0.0566(9)	0.5867(2)	1.0(—)	0.0081(5)

^aAlternative model (see text), 1: 0.938(4), 2: 0.009(1), 3: 0.0347(6). ^bRestraints used (see text). ^cPosition not refined, in order to define origin along *a*.

Table 4 Details of structure refinements

	Bi ₂ BaNb ₂ O ₉	Bi ₂ SrNb ₂ O ₉	Bi ₂ CaNb ₂ O ₉
crystal system	tetragonal	orthorhombic	orthorhombic
space group	<i>I4/mmm</i>	<i>A2₁am</i>	<i>A2₁am</i>
cell parameters			
<i>a</i> /Å	3.9362(1)	5.5193(3)	5.4833(1)
<i>b</i> /Å		5.5148(3)	5.4423(1)
<i>c</i> /Å	25.6582(7)	24.0857(6)	24.8984(6)
absorption factor (<i>μ</i> t)	1.6	1.7	1.8
structure refinement:			
X-ray			
2θ range/degrees	10–90	10–90	10–90
no. of reflections	75	187	182
no. of data points	3998	3998	3998
<i>R</i> _{wp} , <i>R</i> _p (%)	12.40, 9.29	12.48, 9.21	14.33, 10.64
<i>R</i> _{wp} ^a , <i>R</i> _p ^a (%)	12.51, 9.34	12.25, 9.04	13.79, 10.25
neutron			
<i>d</i> -spacing range	0.4688–4.016	0.4554–4.016	0.5972–4.016
no. of reflections	697	2371	1057
no. of data points	5299	5319	5109
<i>R</i> _{wp} , <i>R</i> _p (%)	9.91, 6.80	10.16, 6.16	9.70, 6.57
<i>R</i> _{wp} ^a , <i>R</i> _p ^a (%)	9.76, 6.69	9.99, 6.03	9.69, 6.55
no. of parameters	36/37 ^a	58/59 ^a	54/55 ^a
combined <i>χ</i> ²	3.72/3.68 ^a	7.02/6.78 ^a	5.71/5.52 ^a

^aAlternative model (see text).

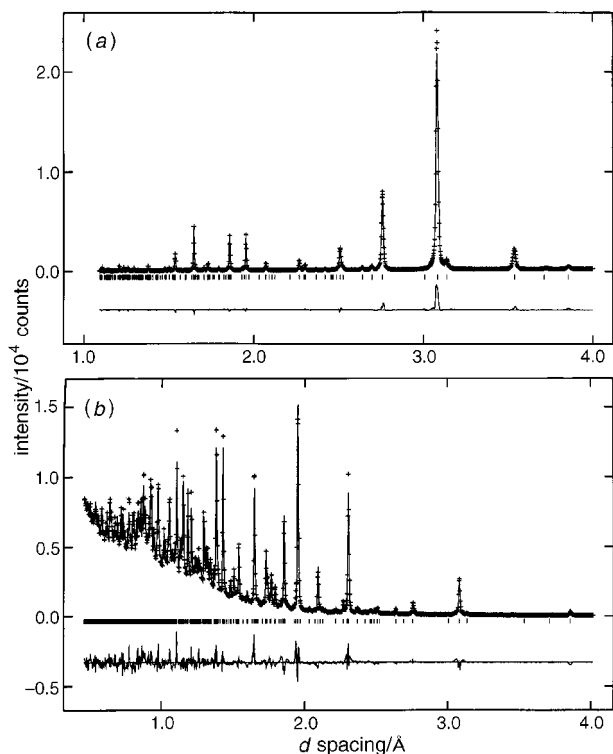


Fig. 2 Final Rietveld fit for $\text{Bi}_2\text{SrNb}_2\text{O}_9$ using (a) X-ray data and (b) neutron data

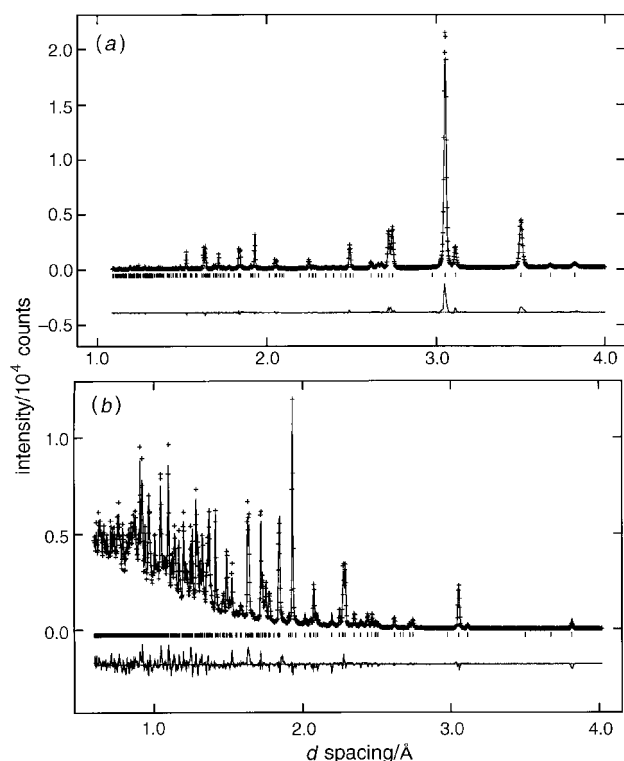


Fig. 3 Final Rietveld fit for $\text{Bi}_2\text{CaNb}_2\text{O}_9$ using (a) X-ray data and (b) neutron data

normally be perceived as more likely to substitute the bismuth site.

Examination of the bond distances in Table 5 shows that the coordination number of the A site can best be described as eight in the strontium and calcium compounds whereas the barium compound can be regarded as twelve coordinate, based on the sum of the relevant ionic radii. The coordination around the A site cation also becomes increasingly distorted. Apparent

bond valence calculations¹⁴ using these bond distances are presented in Table 6. It can be seen that the calculated valence of the A site cation is larger than two in all the compounds and therefore that 'overbonding' of the A site cation occurs. It is also evident that the calculated valence of the A site cation decreases as the cation size decreases, implying that the overbonding is alleviated as the cation size decreases. Overbonding of the A site cation appears to be inherent in two-layer Aurivillius compounds with a divalent cation occupying the A site, *i.e.* the apparent valence of the quenched sample of $\text{Bi}_2\text{PbNb}_2\text{O}_9$ was 2.57, and the apparent valence of $\text{Bi}_2\text{SrTa}_2\text{O}_9$ was 2.37. Only in the two-layer Aurivillius phase, $\text{Bi}_3\text{NbTiO}_9$, has the A site cation valence been reported to be underbonded and in this case the cation is trivalent.⁵

The effect of cation disordering is to reduce the overbonding of the A site cation in the barium and strontium case. It is interesting to note that the cation disorder actually increases the apparent valence of the A site cation in the calcium case. It is possible that there is an 'optimum' apparent valence for the A site cation in these phases, *i.e.* a degree of overbonding is necessary to stabilise the Aurivillius structure.

The apparent valence of the bismuth site increases as the A site cation size decreases. In this site, the cation disorder serves to reduce the 'underbonding' of the bismuth site in the barium and strontium compounds.

It is also apparent from the bond distances in Table 5 that the niobium becomes less displaced along the axial direction as the cation size decreases. The niobium atom is slightly underbonded in all of these compounds.

It seems that there are two effects occurring as a function of cation size. The structure becomes more distorted as the cation size decreases, *i.e.* the Ca atom, despite being slightly 'overbonded', is too small for the A site, leading to the rotation and tilting of the niobium octahedra which results in the orthorhombic distortion. The Ba atom is the most overbonded cation and it actually is too large for the A site, hence it exhibits the most cation disordering with the smaller bismuth cation.

Conclusions

Simultaneous X-ray and neutron powder refinements have been used to obtain accurate models of the structures of $\text{Bi}_2\text{BaNb}_2\text{O}_9$, $\text{Bi}_2\text{SrNb}_2\text{O}_9$ and $\text{Bi}_2\text{CaNb}_2\text{O}_9$. All the compounds exhibit disorder between the bismuth and A sites, increasing as the A site cation size increases. The cause of the disorder may be explained by a combination of cation size considerations and bond valence sum analysis, *i.e.* the Ba atom is too big for occupation of the A site, leading to bismuth:A site disordering, whereas the Ca atom is too small for the A site, resulting in a large orthorhombic distortion. The ideal value of the bond valence for a divalent cation in an Aurivillius structure of this type is probably in the region of 2.3–2.4. It is possible that the two-layer Aurivillius structure may prefer a trivalent cation on the A site, therefore a structural study of $\text{Bi}_2\text{LnNbTiO}_9$ ($\text{Ln} = \text{La} - \text{Lu}$) would be apposite, to determine whether any cation disordering would occur for the lanthanide series.

It is interesting to note that the two-layer Aurivillius phase niobates have higher Curie temperatures than the corresponding tantalates.³ In this study, $\text{Bi}_2\text{SrNb}_2\text{O}_9$ exhibits cation disorder and a more distorted niobium octahedral environment than the $\text{Bi}_2\text{SrTa}_2\text{O}_9$ model reported by Withers. Further work is required to determine whether these factors contribute to the observed differences in the Curie temperatures.

We would like to thank SERC and the University of St. Andrews for funding. We wish to acknowledge the use of the EPSRC's Chemical Database Service at Daresbury.¹⁵ This work has also benefited from the use of the Intense Pulsed

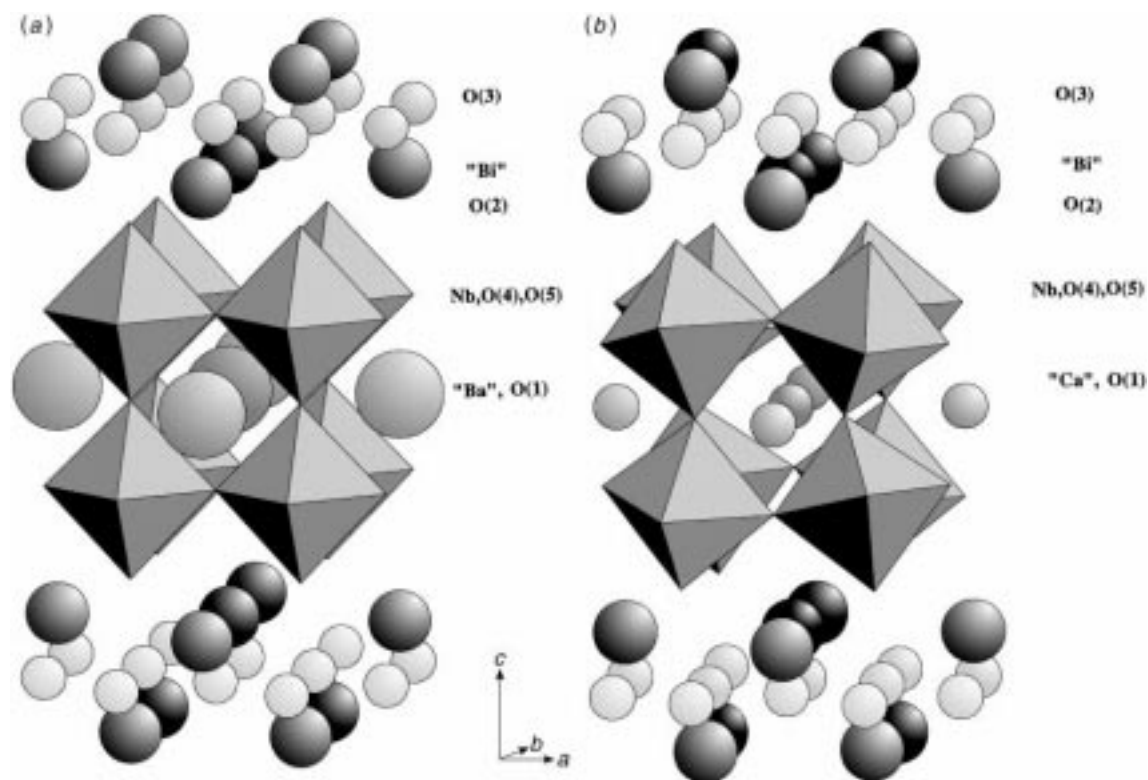


Fig. 4 Perspective drawing of (a) undistorted $\text{Bi}_2\text{BaNb}_2\text{O}_9$ and (b) $\text{Bi}_2\text{CaNb}_2\text{O}_9$ from $\frac{1}{4}c$ to $\frac{3}{4}c$

Table 5 Bond distances/Å

bond type	$\text{Bi}_2\text{BaNb}_2\text{O}_9$	$\text{Bi}_2\text{SrNb}_2\text{O}_9$	$\text{Bi}_2\text{CaNb}_2\text{O}_9$
$\text{Bi}/\text{A}(1)-\text{O}(1)$	$2.7833(1) \times 4$	2.98(1) 2.96(2) 2.57(2) 2.55(1)	3.155(9) 3.12(1) 2.43(1) 2.334(9)
$\text{Bi}/\text{A}(1)-\text{O}(4)$	$2.810(1) \times 8$	$2.698(9) \times 2$ $2.58(1) \times 2$	$2.610(8) \times 2$ $2.378(8) \times 2$
$\text{Bi}/\text{A}(1)-\text{O}(5)$	—	$3.162(8) \times 2$ $2.640(7) \times 2$	$3.325(7) \times 2$ $2.545(6) \times 2$
$\text{Bi}/\text{A}(2)-\text{O}(2)$	$2.3069(9) \times 4$	2.626(7) 2.79(1) 3.14(1) 3.307(6) 3.525(4)	2.525(4) 2.729(6) 3.208(6) 3.386(4) 3.610(4)
$\text{Bi}/\text{A}(2)-\text{O}(3)$	$2.992(1) \times 4$	2.174(7) 2.282(7) 2.361(7) 2.391(7) 3.303(5)	2.221(5) 2.261(5) 2.320(6) 2.370(5) 3.164(5)
$\text{Bi}/\text{A}(2)-\text{O}(5)$	—	3.303(5)	3.164(5)
$\text{Nb}-\text{O}(1)$	2.273(2)	2.199(2)	2.156(2)
$\text{Nb}-\text{O}(2)$	1.839(4)	1.832(5)	1.821(4)
$\text{Nb}-\text{O}(4)$	$1.9862(3) \times 4$	2.064(7) 1.885(7)	2.091(6) 1.941(6)
$\text{Nb}-\text{O}(5)$	—	2.058(9) 1.967(8)	2.079(6) 1.918(6)

Table 6 Apparent bond valence

site ^a	$\text{Bi}_2\text{BaNb}_2\text{O}_9$	$\text{Bi}_2\text{SrNb}_2\text{O}_9$	$\text{Bi}_2\text{CaNb}_2\text{O}_9$
$\text{A}_{100\%}$	2.97	2.42	2.23
A_{exp}	2.65	2.39	2.32
$\text{Bi}_{100\%}$	2.60	2.87	3.01
Bi_{exp}	2.84	2.89	2.96
Nb_{exp}	4.86	4.96	4.93

^a $\text{A}_{100\%}$ is apparent valence of the A site assuming full occupation by A. A_{exp} is apparent valence of the A site assuming experimentally observed occupation.

Neutron Source at Argonne National Laboratory which is funded by the US Department of Energy, BES-Materials Science, under Contract W-31-109-ENG-38. We thank Dr J. D. Jorgensen and S. Short for collecting the neutron data.

References

- 1 B. Aurivillius, *Arki. Kemi.*, 1949, **1**, 463.
- 2 G. A. Smolenski, V. A. Isupov and Agranovskaya, *Sov. Phys. Solid State (Engl. Transl.)*, 1959, **3**, 651.
- 3 E. C. Subbarao, *J. Phys. Chem. Solids*, 1962, **23**, 665.
- 4 A. D. Rae, J. G. Thompson, R. L. Withers and A. C. Willis, *Acta Crystallogr., Sect. B*, 1991, **47**, 174.
- 5 J. G. Thompson, A. D. Rae and R. L. Withers, D. C. Craig, *Acta Crystallogr., Sect. B*, 1990, **46**, 474.
- 6 A. D. Rae, J. G. Thompson and R. L. Withers, *Acta Crystallogr., Sect. B*, 1992, **48**, 418.
- 7 C. A-Paz de Araujo, J. D. Cuchlaro, L. D. McMillan, M. C. Scott and J. F. Scott, *Nature (London)*, 1995, **374**, 627.
- 8 R. L. Withers, J. G. Thompson and A. D. Rae, *J. Solid State Chem.*, 1991, **94**, 404.
- 9 Ismunandar, B. J. Kennedy, Gunawan and Marsongkohadi, *J. Solid State Chem.*, 1996, **126**, 135.
- 10 V. Srikanth, H. Idink, W. B. White, E. C. Subbarao, H. Rajagopal and A. Sequeira, *Acta Crystallogr., Sect. B*, 1996, **52**, 432.
- 11 P. Millan, A. Castro and J. B. Torrance, *Mater. Res. Bull.*, 1993, **28**, 117.
- 12 J. D. Jorgensen, J. Faber Jr., J. M. Carpenter, R. K. Crawford, J. R. Haumann, R. L. Hitterman, R. Kleb, G. E. Ostrowski, F. J. Rotella and T. J. Worlton, *J. Appl. Crystallogr.*, 1989, **22**, 321.
- 13 A. C. Larson and R. B. von Dreele, Los Alamos National Laboratory Report No. LA-UR-86-748, 1987.
- 14 I. D. Brown and D. Altermatt, *Acta Crystallogr., Sect. B*, 1985, **41**, 244.
- 15 The United Kingdom Chemical Database Service, D. A. Fletcher, R. F. McMeeking and D. Parkin, *J. Chem. Inf. Comput. Sci.*, 1996, **36**, 746.

Paper 6/08059F; Received 28th November, 1996